

2007

Physical Phenomena in Electronic Materials in the Terahertz Region

R. A. Lewis

University of Wollongong, roger@uow.edu.au

Publication Details

This article was originally published as Lewis, RA, Physical Phenomena in Electronic Materials in the Terahertz Region, Proceedings of the IEEE, 95(8), 2007, 1641-1645. Copyright 2007, IEEE.

Research Online is the open access institutional repository for the University of Wollongong. For further information contact the UOW Library: research-pubs@uow.edu.au

Physical Phenomena in Electronic Materials in the Terahertz Region

Terahertz radiation is useful for probing electronic materials because energies, resonances and other key physical characteristics of these materials correspond to THz frequencies.

By R. A. LEWIS

ABSTRACT | Terahertz radiation is a powerful probe of materials' properties, because many materials have characteristic energies corresponding to the energies of terahertz photons. Take the particular example of semiconductor materials: phonon energies, cyclotron energies, and the energy levels of bound states in quantum wells, all typically lie in the terahertz region. Contrariwise, the properties of materials are crucial in the development of terahertz technology. This applies to every part of the system—from emitter, through elements for transferring and manipulating the radiation, and finally to the detector.

KEYWORDS | Far-infrared; T-ray; terahertz; THz

I. PHYSICAL PHENOMENA IN THE TERAHERTZ REGION

The region of the electromagnetic spectrum corresponding to terahertz (THz, 10^{12} cycles per second) frequencies is of great scientific and technical interest in view of the number of physical phenomena that are found there. We will consider several of these, with a particular emphasis on phenomena in crystalline solids, especially semiconductors.

A. Boltzmann Energy

The Boltzmann energy, twice the thermal energy per degree of freedom, is given by

$$E = k_B T \quad (1)$$

where T is the absolute temperature (K) and k_B is the Boltzmann constant [1]

$$k_B = 0.020836644(36) \text{ THz K}^{-1} \quad (2)$$

$$= 0.08617343(15) \text{ meV K}^{-1}. \quad (3)$$

The Boltzmann energy (in units of milli-electron-volts) and corresponding photon frequency (in units of terahertz) for several temperatures are given in Table 1. The technologically important temperatures of the boiling points of helium, nitrogen, and water at standard pressure; the triple point of water; and room temperature, are included. It may be seen that the “terahertz regime,” in the sense of frequency f in the range $0.1 \text{ THz} < f < 10 \text{ THz}$, runs from almost the boiling point of liquid helium to a little above room temperature, spanning the most technically important temperature range.

B. Shallow Impurities in Semiconductors: The Effective-Mass Approximation

Group V (donor) or Group III (acceptor) foreign atoms introduced into the lattice of a Group IV elemental semiconductor such as Si or Ge introduce either an electron or a hole which orbits the ion core in much the same way that an electron orbits the proton in the hydrogen atom. The energy levels are calculated within the “effective-mass

Manuscript received November 1, 2005; revised March 10, 2007. This work was supported in part by the Australian Research Council and in part by the University of Wollongong.

The author is with the Institute for Superconducting and Electronic Materials and the School of Engineering Physics, University of Wollongong, Wollongong, NSW 2522, Australia (e-mail: roger@uow.edu.au).

Digital Object Identifier: 10.1109/JPROC.2007.898902

Table 1 The Frequency (THz) of a Photon of Given Boltzmann Energy (meV) for Several Temperatures (K)

	Temperature T (K)	Frequency f (THz)	Energy E (meV)
One Kelvin	1	0.020836644	0.08617343
He boils	4.2	0.088	0.36
	10	0.20836644	0.8617343
One meV	11.60451	0.24179894	1
	20	0.41673288	1.723469
One THz	47.992373	1	4.135667
	50	1.0418322	4.308672
N boils	77.4	1.61	6.67
	100	2.0836644	8.617343
	200	4.1673288	17.23469
Water boils	273.15	5.6915	23.538
Triple point	273.16	5.6917	23.539
Room temperature	293.15	6.1083	25.262
	300	6.2509932	25.85203
	500	10.418322	43.08672

approximation” by replacing the mass of the electron m_e with the effective mass m^* and scaling by the dielectric constant of the lattice ϵ . The effective Rydberg of the hydrogenic system is

$$Ry^* = \frac{m^*}{m_e} \frac{1}{\epsilon^2} Ry. \quad (4)$$

Since the effective mass tends to be smaller than the electron mass and the dielectric constant of the semiconductor host is larger than that of the vacuum, the characteristic energies are much reduced in the solid-state analog of the hydrogen atom compared to the hydrogen atom itself and so the energies of transitions between states are typically not of the order of an eV, but rather of the order of an meV; in other words, corresponding to the energies of photons with THz frequencies. For example, the Sb donor in Ge has an ionization energy of about 9.6 meV, corresponding to a photon of about 2 THz. While such transitions have been studied for many years, they are of continuing interest. For example, the P donor in Si has been proposed by Kane as the basis of a quantum computer [2]. Hydrogenic transitions in a sample of Si rather heavily doped with P are shown in Fig. 1. The lowest energy hydrogenic transition, $1s \rightarrow 2p_0$, occurs at 8.2 THz.

C. Confined Levels in Semiconductor Heterostructures

From elementary quantum mechanics, the energy of the n th allowed state of a particle of mass m confined to a region of length a is

$$E_n = \frac{h^2 n^2}{8ma^2} \quad (5)$$

where h is Planck’s constant. If we consider a typical case of an electron of effective mass $m^* = 0.067m_e$ in GaAs confined to a layer of width 10 nm, we obtain the ground-state energy $E_1 = 5.6$ meV, corresponding to photons of frequency 1.4 THz.

D. The Effect of a Magnetic Field on Free Carriers: Cyclotron Resonance (cr)

When a charge carrier has a component of velocity perpendicular to a magnetic field B , it circles the field at the cyclotron frequency

$$\omega_{cr} = \frac{eB}{m^*}. \quad (6)$$

For semiconductors in laboratory magnetic fields, the cyclotron frequency is typically in the THz range; for example, in n -GaAs, f_{cr} varies as 0.42 THz per Tesla. The characteristic magnetic length is

$$L = \sqrt{\frac{\hbar}{eB}} \quad (7)$$

which has a numerical value of $(257 \text{ \AA} T^{1/2})/\sqrt{B}$. While the frequency of the resonance in a known field yields the effective mass of the charge carriers, the width of the resonance yields the (optical) mobility

$$\mu_{cr} = \frac{e\tau_{cr}}{m^*} \quad (8)$$

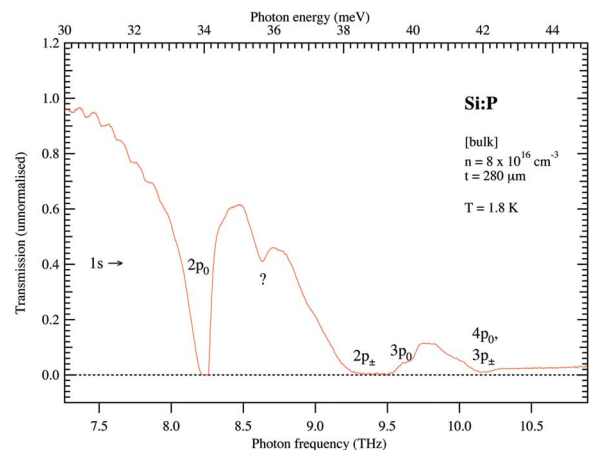


Fig. 1. Spectrum of P donor impurity in Si. (The origin of the feature marked “?” is not known.)

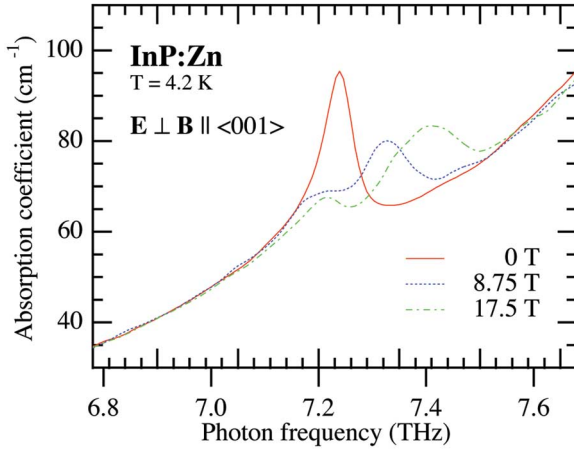


Fig. 2. Spectrum of Zn acceptor impurity in InP in the region of the lowest-energy transition from the ground state, the “G line,” for three magnetic fields.

where the scattering time $\tau_{cr} = 2Q/\omega_{cr}$ is determined from the quality factor $Q = B_{cr}/\Delta B$, where ΔB is the full width at half-maximum (FWHM) of the resonance.

As an example of the detail available in such studies, cyclotron resonance has been detected by THz photoconductivity in the two-dimensional electron gas formed in undoped, top-gated GaAs/Al_{0.3}Ga_{0.7}As heterostructures [3]. A cyclotron frequency $f_{cr} = 1.6$ THz was observed at field $B_{cr} = 3.93$ T, and so the electron cyclotron mass is $0.068m_e$. The full widths at half maximum were 15 mT at 4.2 K and 6 mT at 1.6 K, corresponding to quality factors of 260 at the higher temperature and 660 at the lower, with corresponding scattering times of 51 and 130 ps, and optical mobilities 1.3 and 3.3×10^6 cm² V⁻¹ s⁻¹ at 4.2 K and 1.6 K, respectively. The extremely high optical mobility was consistent with the low-field ballistic focusing observed in magnetotransport in this and similar samples, exceeding that of the best bulk samples. The cyclotron resonance was studied as a function of filling factor $\nu (= n_s h/eB)$ for $0.2 < \nu < 5$ and maxima in linewidth were observed at even filling factors ($\nu = 2, 4, 6$). In the quantum limit the FWHM will vary with density according to

$$\Delta B = \delta B + 2m^*\omega_p/e \quad (9)$$

where ΔB is the experimental and δB the true FWHM, ω_p is the plasma frequency, given by $\omega_p^2 = Z_0 n_s e^2 / m^* (1 + \sqrt{\epsilon})$, Z_0 is the impedance of free space, and $\epsilon = 12.56$ is the dielectric constant of GaAs. The effective mass was measured for a range of THz laser energies and found to increase with increasing energy due to band nonparabolicity. The dependence is given by the equation $m^* =$

m_0^* , where m_0^* is the cyclotron mass extrapolated to $B = 0$, E_g is the band gap of GaAs ($= 1519$ meV), and $K_2 = -1.8$ is a constant determined by a fit to the data.

E. The Effect of a Magnetic Field on Bound Carriers: Zeeman Effect

Just as the electron states in atomic hydrogen undergo Zeeman splitting in a magnetic field, the electronic states in the solid-state analog of shallow impurities in semiconductors do also. The situation regarding donors is generally rather straightforward, especially if the conduction band is isotropic and the conduction band minimum at the zone center. The situation regarding acceptors is more interesting in view of the more complex character of the valence band and will be considered further. The effect of a magnetic field on different hydrogenic systems is conveniently described via a dimensionless unit for the magnetic field strength, the ratio of the magnetic energy $\mu_B B$ (μ_B is the Bohr magneton, B the magnetic field) to the Rydberg energy Ry . This ratio is unity at the magnetic field

$$B_0 = \frac{Ry}{\mu_B} \quad (10)$$

which has the value of 235 052 T. For an acceptor of first Luttinger parameter γ_1 in a semiconductor of dielectric constant ϵ , the effective Rydberg $Ry^* = Ry/\gamma_1 \epsilon^2$ and the effective Bohr magneton $\mu_B^* = \gamma_1 \mu_B$; so

$$B_0^* = \frac{1}{\gamma_1 \epsilon^2} \frac{Ry}{\mu_B}. \quad (11)$$

Recently the cases of Be acceptor in GaAs [4] and Zn acceptor in InP [5]–[7] have been investigated in detail.

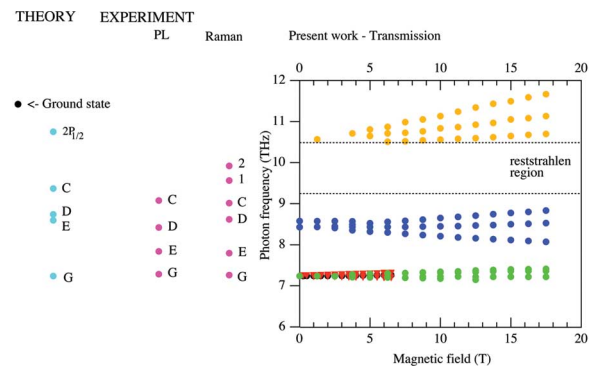


Fig. 3. Development of Zn acceptor impurity in InP transitions with magnetic field.

For these cases, B_0^* is 34 T and 58 T, respectively. In Fig. 2 it is seen that the effect of the magnetic field is to shift and split the original transition. The development of three transitions with magnetic field is shown in Fig. 3, which also contains the energies of the transitions in the absence of magnetic field as determined by calculations and by photoluminescence (PL) and Raman spectroscopy. The theoretical splittings vary with the symmetry of the initial and final states and with the orientation of the crystal with respect to the magnetic field, but with field parallel to a $\langle 001 \rangle$ crystal axis, the energies of the four sublevels of a Γ_8 state are given by

$$E_m^p = \mu_B (mg_1^p + m^3 g_2^p) B + [q_1^p + (q_2^p + q_3^p) m^2] B^2 \quad (12)$$

where $m = \pm(1/2), \pm(3/2)$ is a spin quantum number characterizing the state within the T_d notation, g and q are materials' parameters, and p labels the particular Γ_8 state. Detailed analysis of the spectra has allowed the g factors to be determined for the ground state and the first excited state [6]. Measurements to very high field have revealed a series of free-hole transitions (Landau-level series) as well as phonon replicas of this and of the more common bound-hole transitions (Lyman series) [7].

F. Phonon Energies

In many electronic materials, phonon frequencies lie in the THz region. For example, in GaAs the optical and acoustic phonon frequencies are of the order of 0.8 and 0.5 THz, respectively [8]. The damped harmonic oscillator dielectric function combined with the free-carrier term is

$$\epsilon(\omega) = \epsilon(\infty) + \frac{\omega_t^2 (\epsilon(0) - \epsilon(\infty))}{\omega_t^2 - \omega^2 + i\gamma\omega} - \frac{\epsilon(\infty)\omega_p^2}{(\omega^2 + i\gamma_p\omega)} \quad (13)$$

$$= \epsilon_1(\omega) + i\epsilon_2(\omega) \quad (14)$$

$$= (n + i\kappa)^2 \quad (15)$$

where ω_t is the TO phonon frequency, γ the phonon damping term, ω_p the plasma frequency, and γ_p the plasma damping term. From the refractive index n and the extinction coefficient κ , the reflectance is calculated using

$$R = \frac{(n-1)^2 + \kappa^2}{(n+1)^2 + \kappa^2}. \quad (16)$$

The plasma term plays a key role and allows the charge-carrier density N to be determined through $\omega_p^2 = Ne^2 / \epsilon(\infty)\epsilon_0 m^*$ [9]. Thus THz reflectivity spectra of undoped polar materials yields the TO and LO phonon energies as

well as the dielectric constant and damping terms. Moreover, the charge carrier concentration may be determined by this purely optical method.

Recently the electronic properties of oxide materials have been under intense scrutiny in view of their technologically important behaviors such as superconductivity and colossal magnetoresistance. One interesting series of perovskites is the cobaltite/manganites, $A(\text{Co}_{1/2}\text{Mn}_{1/2})\text{O}_3$, where A is a lanthanide. THz spectroscopy demonstrates that the phonon modes split and shift as the radius of the lanthanide on the A site decreases, which correlates with the appearance of metamagnetism in the series [10]. In strong magnetic field, the phonon frequencies for $A = \text{La}, \text{Nd}, \text{and Ho}$ show little change, whereas they split for $A = \text{Yb}$. This is thought to be related to the metamagnetism of $\text{Yb}(\text{Co}_{1/2}\text{Mn}_{1/2})\text{O}_3$ [11].

G. Other Interactions

THz spectroscopy is also a valuable probe of more complex interactions, such as the electron–phonon interaction. The coupling of a zone-center phonon with a bound-state to bound-state transition results in a “Fano resonance,” the general description of a discrete state being in resonance with a continuum of states [12]. The magnetopolaron interaction is another example, which recently has been investigated to high magnetic field in $n\text{-InP}$ [13]. Interactions involving more particles have been calculated and observed—for example, magnetophonon resonances accompanied by cyclotron resonances [14]. A splitting of the cyclotron resonance peak is attributed to magnetophoton–phonon scattering.

II. MATERIALS IN TERAHERTZ TECHNOLOGY

It has been shown that many materials' properties, particularly the states of electrons, of phonons, and their interactions, may be investigated by the absorption or reflection of THz radiation by them. On the other hand, materials' properties play a crucial role in the development of the technology that allows such investigations to be conducted [15].

THz technology has been reviewed by Siegel [16]. At every stage in the particular technique of terahertz time-domain spectroscopy (THz-TDS), materials' properties are important and impact on the efficiency and convenience of use of the apparatus. At the outset, the efficiency and bandwidth of the emitter are determined by the physical mechanism of conversion of near-infrared (NIR) light pulses to THz radiation, for example by electrooptic rectification or by photoconductivity, and these depend in turn on such properties as the nature and amount of impurities in the emitter. The most common unbiased emitter has been $\langle 110 \rangle$ ZnTe. Recently, p -type InAs has been shown to be a strong emitter of THz radiation [17], [18]. The mechanism of THz generation depends on

charge-carrier diffusion [19]. The most common photoconductive emitter is now low-temperature grown GaAs [20]. Just as the emitter efficiency depends strongly on the physical properties of the emitter material, the sensitivity and bandwidth of the detector is controlled by such factors as the geometry and purity of the detector material. THz waveguides produce a further materials challenge [21]. Another important consideration in a typical THz-TDS system is the filtering to block NIR radiation but at the same time transmit THz radiation. The distinction may be made between the mechanism of scattering, important when the material is placed near the source, and absorption, important when the material is placed near the detector. There are many materials which transmit well in the THz region and so are useful, for example for cryostat windows, but are not effective in blocking NIR radiation. These materials include mylar, polypropylene, TPX, and polyethylene. It has been found that, when placed close to a detector, these block only 6%, 45%, 73%, and 95% of the incident NIR, respectively. Materials that block 99% or more of the NIR but also transmit well in the

THz include filter paper, teflon, polystyrene, and silicon. While Si does not pass as much radiation as the other materials at the lowest frequencies (due to reflection at the front face as a consequence of its high refractive index) it has a very uniform profile across the frequency range, and becomes better than the organic materials as the frequency increases.

III. CONCLUSION

THz technology provides an excellent probe of the physical properties of electronic materials and in turn depends crucially on electronic materials' properties. ■

Acknowledgment

The author would like to thank many present and former students and colleagues who have contributed to the work discussed here. These include C. Zhang, R. E. M. Vickers, R. Mendis, M. L. Smith, L. J. Bignell, and S. Hargreaves.

REFERENCES

- [1] CODATA internationally recommended values of the fundamental physical constants, 2002. [Online]. Available: <http://www.physics.nist.gov/cuu/Constants/index.html>
- [2] B. E. Kane, "A silicon-based nuclear spin quantum computer," *Nature*, vol. 393, pp. 133–137, 2000.
- [3] R. J. Heron, R. A. Lewis, R. G. Clark, R. P. Starrett, B. E. Kane, G. R. Facer, N. E. Lumpkin, D. G. Rickel, L. N. Pfeiffer, and K. W. West, "Cyclotron resonance in undoped, top-gated heterostructures," *Semicond. Sci. Tech.*, vol. 15, pp. 589–592, 2000.
- [4] R. A. Lewis, Y.-J. Wang, and M. Henini, "Magneto-spectroscopy of Be in GaAs," *Phys. Rev. B*, vol. 67, p. 235 204, 2003.
- [5] R. L. Causley and R. A. Lewis, "Far-infrared spectroscopy of the zinc acceptor in indium phosphide," *Physica B*, vol. 302–303, pp. 327–333, 2001.
- [6] R. A. Lewis and Y. J. Wang, "Zeeman spectroscopy of the Zn acceptor in InP," *Solid State Commun.*, vol. 126, pp. 275–280, 2003.
- [7] R. A. Lewis and Y. J. Wang, "Magneto-optical far-infrared absorption spectroscopy of the hole states of indium phosphide," *Phys. Rev. B*, vol. 71, p. 115 211, 2005.
- [8] W. Xu, "Generation of terahertz acoustic-phonon signals by heated electrons in $\text{Al}_x\text{Ga}_{1-x}\text{As}/\text{GaAs}$ -based quantum wires," *Appl. Phys. Lett.*, vol. 68, pp. 1353–1355, 1996.
- [9] R. L. Causley and R. A. Lewis, "Characterisation of indium phosphide using terahertz radiation," in *Proc. 2000 International Semiconducting and Insulating Materials Conf.*, pp. 101–104.
- [10] F. Gao, R. A. Lewis, X. L. Wang, and S. X. Dou, "Phonon modes of $\text{A}(\text{Co}_{1/2}\text{Mn}_{1/2})\text{O}_3$ ($\text{A} = \text{La, Nd, Dy, Ho, Yb}$)," *J. Solid State Chem.*, vol. 160, pp. 350–352, 2001.
- [11] R. A. Lewis, Y.-J. Wang, F. Gao, X. L. Wang, and S. X. Dou, "Phonon spectra of cobaltite/manganites in strong magnetic fields," *J. Magn. Magn. Mater.*, vol. 272–276, pp. 616–617, 2004.
- [12] G. Piao, P. Fisher, and R. A. Lewis, "Piezospectroscopy of the $p_{3/2}$ and Fano series of singly ionized zinc in germanium," *Phys. Rev. B*, vol. 61, pp. 7466–7478, 2000.
- [13] R. A. Lewis, P. E. Simmonds, and Y. J. Wang, "Magneton interactions in n -type indium phosphide," *Phys. Rev. B*, vol. 72, p. 245 207, 2005.
- [14] W. Xu, R. A. Lewis, P. M. Koenraad, and C. J. G. M. Langerak, "High-field magnetotransport in a two-dimensional electron gas in quantizing magnetic fields and intense terahertz laser fields," *J. Phys.: Condens. Mat.*, vol. 16, pp. 89–101, 2004.
- [15] B. Ferguson and X.-C. Zhang, "Materials for terahertz science and technology," *Nature Mater.*, vol. 1, pp. 26–33, 2002.
- [16] P. H. Siegel, "Terahertz technology," *IEEE Trans. Microwave Theory Tech.*, vol. 50, no. 3, pp. 910–928, Mar. 2002.
- [17] R. Adomavičius, A. Urbanowicz, G. Molis, A. Krotkus, and E. Šatkovskis, "Terahertz emission from p -InAs due to the instantaneous polarization," *Appl. Phys. Lett.*, vol. 85, pp. 2463–2465, 2004.
- [18] R. A. Lewis, M. L. Smith, R. Mendis, and R. E. M. Vickers, "THz generation in InAs," *Physica B*, vol. 376–377, pp. 618–621, 2006.
- [19] K. Liu, J. Xu, T. Yuan, and X.-C. Zhang, "Terahertz radiation from InAs induced by carrier diffusion and drift," *Phys. Rev. B*, vol. 73, no. 15, p. 155 330, 2006.
- [20] I. S. Gregory, C. Baker, W. R. Tribe, M. J. Evans, H. E. Beere, E. H. Linfield, A. G. Davies, and M. Missous, "High resistivity annealed low temperature GaAs with 100 fs lifetimes," *Appl. Phys. Lett.*, vol. 83, pp. 4199–4201, 2003.
- [21] K. Wang and D. M. Mittleman, "Metal wires for terahertz wave guiding," *Nature*, vol. 432, pp. 376–379, 2004.

ABOUT THE AUTHOR

R. A. Lewis received the B.Sc. (Hons) degree from the University of Sydney, Australia, and the Ph.D. degree from Griffith University, Brisbane, Australia.

He is the Head of the School of Engineering Physics and a member of the Institute for Superconducting and Electronic Materials at the University of Wollongong, Wollongong, Australia. His current research interests include terahertz spectroscopy and thermionics.

Prof. Lewis is a Fellow of the Australian Institute of Physics and of the Royal Microscopical Society.

